Engineering Science & Technology
https://ojs.wiserpub.com/index.php/EST/

UNIVERSAL WISER PUBLISHER

Research Article

Identification of Optimized Spot Welding Parameters for Advanced Automotive Steels

Amarjeet Kumar Singh*, D. Satish Kumar

JSW Steel Ltd., Vijaynagar Works, Bellary, Karnataka, 583123, India
E-mail: amarjeet.singh1@jsw.in

Received: 8 January 2025; **Revised:** 7 July 2025; **Accepted:** 14 July 2025

Abstract: Due to the increasing demand to reduce weight-to-strength ratios in the automotive industry, the use of Advanced High Strength Steel (AHSS) materials has grown significantly. In automotive assembly, a number of components are welded to achieve structural stability, making the weldability of the materials a critical aspect in their design and selection. Therefore, in this study, commonly used automotive steel grades-IF 270, TRIP 690, DP 780, and TRIP 980 materials-were selected, and a welding study was conducted. Since a welding experiment is time- and resource-consuming, a simulation method was developed. A model incorporating thermo-mechanical and metallurgical phenomena was developed using SYSWELD software (a welding and heat treatment simulation software by ESI Group) to simulate the resistance spot welding processes. This study provides critical current value mappings for various phenomena during resistance spot welding of automotive-grade steels. It was observed that, with the increase in welding current, weld diameter and failure load increase before expulsion. Predictions of nugget size and Heat-Affected Zone (HAZ) using the developed model match well with experimental results.

***Keywords*:** spot welding, Finite Element Method (FEM) simulation, AHSS, SYSWELD

1. Introduction

Resistance Spot Welding (RSW) is a widely used technique for joining thin steel and aluminum sheets, particularly in the automotive industry, due to its cost-effectiveness, efficiency, and reliability. Modern automobiles incorporate approximately 4,000 spot welds, making process control and quality assurance crucial to ensuring robust and consistent welds across various applications. To maintain weld quality, optimizing process parameters is essential for each new sheet combination. Traditionally, these parameters are determined through physical experiments, which can be time-consuming and resource-intensive. To improve the efficiency in process planning, simulation software such as SYSWELD has been developed. This study evaluates the effectiveness of SYSWELD in meeting industrial application requirements by analyzing its accuracy and reliability in simulating resistance spot welding processes.

SYSWELD accurately simulates the physical phenomena of welding through thermal analysis based on a transient thermal conduction model. Different welding processes require specific heat source models to represent heat transfer and fusion behavior effectively. Goldak's double ellipsoid heat source is widely used for welding techniques such as Metal Inert Gas (MIG) and Tungsten Inert Gas (TIG), as it provides a realistic approximation of heat distribution [1]. In contrast, high-energy welding processes, such as laser beam and electron beam welding, utilize beam heat sources

DOI: https://doi.org/10.37256/est.6220256372

characterized by a Gaussian temperature distribution, ensuring precise and concentrated heat input modeling [2].

In the International Institute of Welding (IIW) round-robin program comparing computed and experimentally measured residual stresses, the SYSWELD was primarily used to model heat input during the welding process, while the kinematic hardening model was recommended for accurately simulating deformation behavior. The ESI welding engineering software suite includes SYSWELD, a comprehensive tool for simulating heat treatment and weld quality by incorporating key physical phenomena such as phase transformations and mechanical effects. Additionally, WELD PLANNER offers a fast and efficient distortion analysis based on the shrinkage method, integrating pre-processing, a solver, and basic post-processing to streamline the welding simulation workflow [3].

Thermal cycles, non-homogeneous temperature distribution, and thermal gradients induce residual stresses and distortions during the welding process, which can compromise the function and safety of structures. The impact of welding sequence on welding-induced distortion and residual stresses is well understood, as welding sequences influence thermal cycles and temperature history, ultimately inducing residual stress and distortion in weldments. Therefore, optimizing the welding sequence through experimental or numerical methods is crucial for minimizing residual stress and distortion. This approach can also reduce or eliminate the need for Post Weld Heat Treatment (PWHT) while achieving target structural performance [4].

In this work, the optimization of different welding parameters was done using SYSWELD software. Once achieving the optimized parameters, it was used for lab scale trail. Finally, mechanical properties and microstructural characteristics were correlated to establish best practices for welding Advanced High-Strength Steel (AHSS) grades.

2. Finite element modeling of RSW

The Finite Element Method (FEM) is a computational technique used to approximate solutions to partial differential equations, simulating real-world systems. This approach divides the system into smaller elements to better represent varying material properties across the domain. Numerous Finite Element models have been developed to replace physical verification of Resistance Spot Welding (RSW), as physical testing is costly and time-consuming. These models aim to provide a more in-depth understanding of the RSW process. Building an accurate FEM model for RSW requires integrating mechanical, thermal, and electrical models to capture the complex interactions and behaviors during welding.

2.1 *Earlier simulations*

The development of Resistance Spot Welding (RSW) models began in the 1960s with a 1D model focused solely on temperature distribution. This was followed by the introduction of 2D and 2D axisymmetric models, which initially concentrated on temperature distribution before later incorporating both temperature and mechanical coupling [5]. Han et al. [6] incorporated effect of temperature and contact pressure during heat transfer in Resistance Spot Welding (RSW). These early models were based on the Finite Difference Method. In the 1980s, Nied [7] introduced the first Finite Element Method-based models for the RSW Process. Subsequent advancements included models integrating electrical, mechanical, and thermal systems, pioneered by Tsai et al. [8]. Ongoing research has led to the refinement of models featuring enhanced contact conditions, 3D representations, specialized models for steel welding, and the inclusion of metallurgical models [9], [10].

2.2 *Finite element method*

SYSWELD, an FEM-based software, is used for welding simulation in this work. It encompasses thermal, mechanical, and metallurgical aspects of the welding process, as shown in Figure 1.

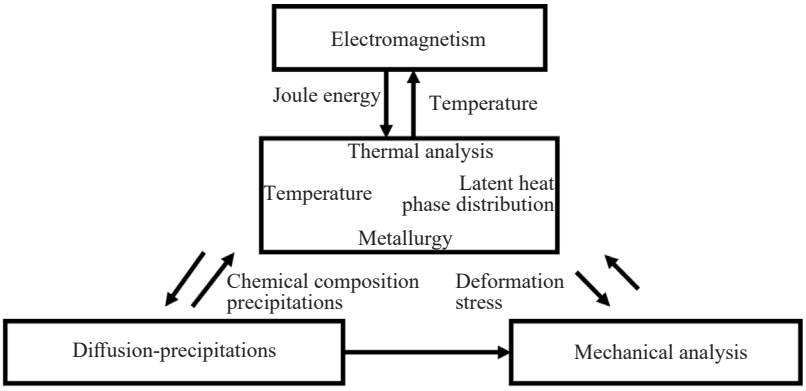

Figure 1. Physics involved in spot welding including mechanical, metallurgical, and thermal aspects

In Resistance Spot Welding (RSW), Finite Element Method (FEM) simulations rely on a coupled electro-thermal-mechanical formulation to accurately predict weld formation. The process begins with the electrical behaviour governed by the steady-state current continuity equation, as given in Equation (1).

$$\nabla \cdot (E(T)\nabla \phi) = 0 \tag{1}$$

$$Q = E\,|\nabla \phi\,|^2 \tag{2}$$

Where ϕ is the electric potential and E is the temperature-dependent electrical conductivity. The resulting Joule heating, which serves as the heat source for the thermal analysis, is given by Equation (2). The thermal behaviour is governed by the transient heat conduction equation (Equation (3)).

$$\rho c_p(T)\frac{\partial T}{\partial t} = \nabla \cdot (k(T)\nabla T) + Q \tag{3}$$

Where ρ is the density, c_p is the specific heat capacity, k is the thermal conductivity, and T is the temperature. Concurrently, the mechanical response of the materials under the applied electrode force and thermal effects is described by the quasi-static equilibrium (Equation (4)).

$$\nabla \cdot \sigma = \rho \frac{\partial^2 u}{\partial t^2} \tag{4}$$

Where σ is the stress tensor, u is displacement vector. To account for melting during welding, the phase change can be included by modifying the effective heat capacity as shown in Equation (5),

$$c_p^{\text{eff}} = c_p + \frac{L}{\Delta T} \tag{5}$$

Where L is the latent heat of fusion and ΔT is the temperature range over which melting occurs. The model also incorporates complex boundary and interface conditions, such as thermal and electrical contact resistance, pressure-dependent heat transfer, and evolving contact areas. Together, these coupled equations given in Table 1 enable the FEM simulation to accurately capture the evolution of temperature fields, nugget growth, and material deformation in the RSW process [11], [12].

Table 1. Governing equations are based on a coupled thermal-electrical-mechanical formulation

Physics	Equation	Role in simulation
Electrical	$\nabla \cdot (E(T)\nabla \phi) = 0$	Determines joule heating source
Thermal	$\rho c_p(T)\frac{\partial T}{\partial t} = \nabla \cdot (k(T)\nabla T) + Q$	Predicts weld nugget growth
Mechanical	$\nabla \cdot \sigma = \rho \frac{\partial^2 u}{\partial t^2}$	Describes deformation, pressure, contact

2.3 *Simulation strategy*

The Finite Element Method (FEM) model setup in SYSWELD for spot welding simulation involves several steps as shown in Figure 2. Below is a guide on how to set up a FEM model for spot welding simulation in SYSWELD:

Geometry and Meshing

• Import or create 3D geometries of the components involved in the spot welding process in Visual Mesh v13.5. This includes the sheets to be welded and the electrodes. In this study, quad linear with collapse Hexa-tetrahedral element was used (Figure 2). The total number of layers mesh is 21. This model consists of 65,000 elements. The element size was 1 mm.

• Generate a suitable mesh for the geometry using a workstation with Intel Xeon processor with 32 GB RAM and Nvidia Graphic card. Ensure that the mesh is fine enough to capture the details of the spot welding process accurately, especially in the weld zone.

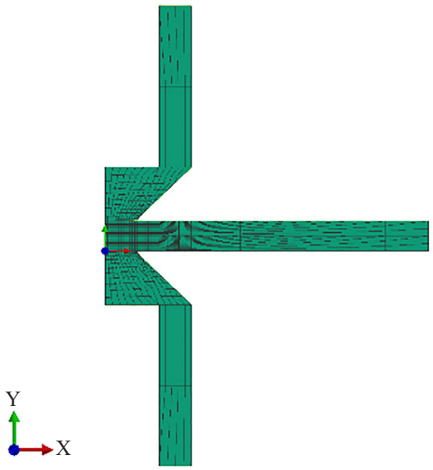

Figure 2. FEA Mesh grids used for electrode and two sheets for spot welding. Fine mesh was used at weld location and larger as moving away from area of interaction

Material Properties

• Define the material properties for the sheets and electrodes. SYSWELD allows the inputs of material data such as thermal conductivity, specific heat, mechanical properties, and more.

Contact and Boundary Conditions

• Define the thermal and electrical contact between the sheets and the electrodes. Joule heating was used for heating the specimen.

• Apply appropriate boundary conditions to represent the physical setup, fixing the sheets or restricting certain degrees of freedom. In this work, the intensity of frequency was defined as 50 Hz, while the squeezing force and squeezing time are

as given in Table 2. However, current was defined in range of 5-15 kA for different grade of steel as given in Table 3.

Table 2. Welding parameters for different grade of steel

Grade	Force (kN)	Squeeze time (cycle)	Welding time (cycle)	Hold time (cycle)
IF	3	60	12-2-12	90
DP 980	5.5	60	12-2-12	90
TRIP 690	4.8	60	12-2-12	90
TRIP 980	5.5	60	12-2-12	90

Table 3. Experimental details for different grade of steel sheet at various current levels

Grade	Current (kA)
IF	5-15
DP 980	5-15
TRIP 690	5-15
TRIP 980	5-15

Thermal Analysis

• Set up the thermal analysis to simulate the heat generation during the spot welding process. Define the welding parameters, such as welding current, time, and electrode force.

• Consider the effects of Joule heating, thermal conduction, and radiation during the welding process.

Coupled Thermal-Mechanical Analysis

• Implement a coupled thermal-mechanical analysis to account for the interaction between temperature and mechanical deformation during the welding process.

• Specify the material's phase transformation behavior, especially if there are phase changes during welding.

Solver Settings

• Choose an appropriate solver within SYSWELD for solving the coupled thermal-mechanical problem. Configure solver settings as total time is 3,000 seconds and time steps for each iteration is 10 seconds.

Post-Processing

• Set up post-processing to analyze and visualize the results. This includes inspecting temperature distributions, stress and strain fields, and the evolution of the weld nugget.

Validation

• Validate the model by comparing simulation results with experimental data if available. Adjust parameters or refine the model as needed to improve accuracy.

Iterate and Optimize

• Iterate the simulation, making adjustments as necessary to improve the accuracy of the model. This may involve refining the mesh, adjusting material parameters, or modifying welding parameters.

3. Experimental details

3.1 *Materials used*

The materials utilized in this investigation consist of various grades of Advanced High-Strength Steel (AHSS).

Specifically, for this study, we employed IF, DP 980, TRIP 980, and TRIP 690 grades, each possessing distinct chemical compositions outlined in Table 1. It is noteworthy that the mechanical properties at the initial conditions are provided in Table 4, offering a comprehensive overview of the material's performance characteristics in its as-received state.

Table 4. Chemical composition of different AHSS grade of steel used as in received conditions

Composition (%) / Grade	C	Mn	Si	Ti	Nb	Cr	Mo	V	Cu	Ni	CE (AWS)
IF	0.002	0.12	0.01	0.03	0.016	0.011	0.001	0.001	0.001	0.008	0.027
DP 980	0.085	3.12	0.202	0.017	0.046	0.022	0.002	0.004	0.006	0.01	0.645
TRIP 690	0.2	1.5	1.2	0.03	0.01	0.018	0.01	0.001	0.006	0.008	0.657
TRIP 980	0.25	2	1.5	0.03	0.04	0.023	0.01	0.001	0.011	0.009	0.841

3.2 *Welding experiment*

The resistance spot welding conditions and parameters for each grade are presented in Table 5. To conduct welding experiments, a spot welding machine fabricated by Amada Miyachi was used in this work. The complete specifications related to the experimental apparatus are provided below:

- Welding Machine Type: IS-800A Amada Miyachi Resistance spot welder.
- Model Number: IS-800A-10-10.
- Machine Capacity:170 Kva/650 V.
- Controller Mode: MFDC.
- Air Cylinder Size: Ø160 × 100 stroke MM.
- Air Cylinder Type: Double.
- Electrode Type: ISO-5821-G.
- Electrode Face Diameter: 8 mm.
- Electrode Face Thickness: 10 mm.
- Cooling Tube OD Diameter: 10 mm.
- Water flow & Temperature: 25 L/Minute & 25 °C.

Once the welding was performed on the selected grade, it was further investigated using SEM for nugget diameter and microstructure formed after welding.

Table 5. Thickness and mechanical properties of different AHSS grade as received

Grade	Thickness	YS (MPa)	UTS (MPa)	EL (%)
IF	1.5	152	296	53.4
DP 980	1.4	714	1,080	13.4
TRIP 690	1.6	444	712	46.14
TRIP 980	1.4	487	945	36

FEM simulation of welding was performed using SYSWELD. The simulation setup procedure, as detailed in the previous section, applies to all welding processes including spot welding. The spot welding simulation in SYSWELD starts from defining the electrode. In this work, the same parameters as experiment were used to run the simulation.

Figure 3 shows different windows during simulation setup. To run the simulation, half side of electrode and specimen was selected, as illustrated in Figure 4.

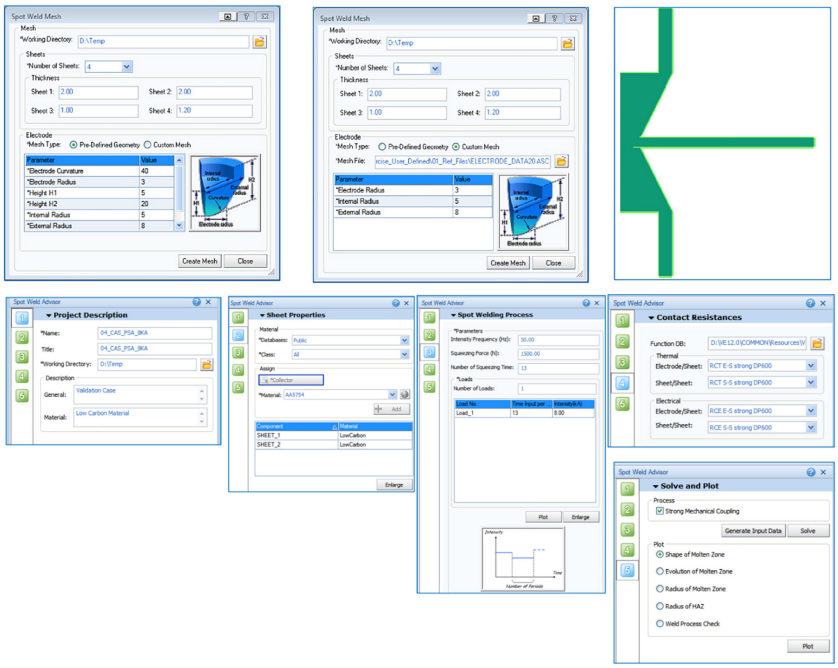

Figure 3. Steps involved in the SYSWELD for setup the simulation

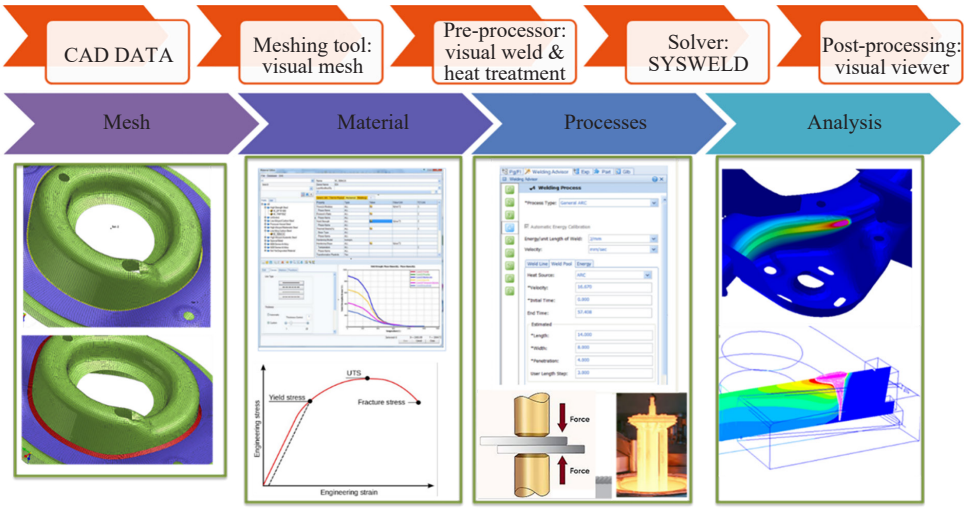

Figure 4. Steps followed in model development in SYSWELD for spot welding consist of meshing of CAD component, input materials property, defining the boundary conditions and analyzed the result

4. Result & discussion

4.1 *Tensile test*

Tensile test of the selected steel grades was performed at room temperature with a constant velocity of 0.08 mm/s. It was observed that IF steel has the maximum elongation and DP-980 has lower elongation. In terms of strength, DP-

980 has higher tensile strength compared to IF steel, as shown in Figure 3.

4.2 *Welding*

Resistance spot welding was performed at different current levels ranging from 5 kA to 10 kA using the experimental setup given in the previous section. After welding was completed, the microstructure and nugget size at different current levels were measured. It was observed that lower current levels led to interfacial fracture, while higher currents resulted in button pull-out failures. All steels demonstrated increased weld diameter and failure load with rising currents until expulsion. Following expulsion, TRIP steels showed continuous growth in electrode indentation, nugget diameter, and weld strength, while DP 780 and IF grades reached a plateau. At expulsion, a sudden decrease in tensile shear strength and nugget diameter was observed for all grades, particularly pronounced in DP 780. The expulsion current range for the selected grades was determined to be 9-10 kA. Welding beyond these values is not recommended, especially for DP 780 and IF grade steel. Nugget size measurement at different currents are shown in Figure 5.

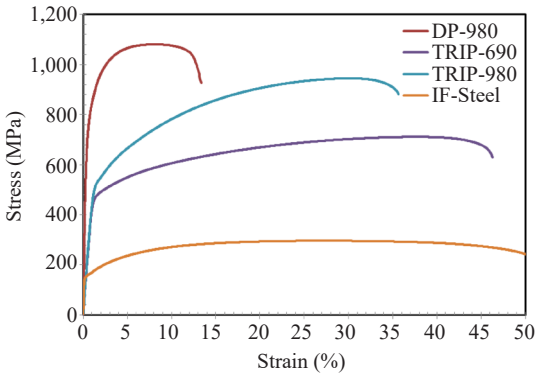

Figure 5. Stress vs strain curve for different AHSS steel grades at room temperature

4.3 *FEM simulation*

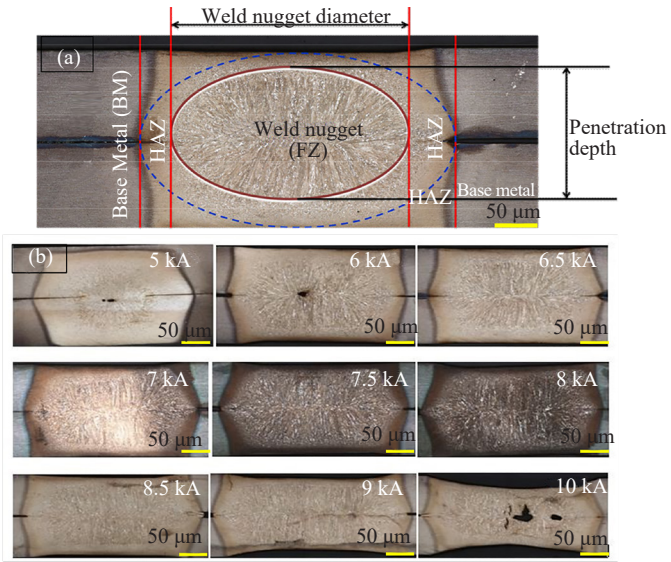

Figure 6. (a) Nugget size measurement at different currents; (b) Nomenclature at different levels of current various from 5 kA to 10 kA for IF steel

It was observed that, with the increase in current, nugget diameter increased for all the selected grades of steel, as shown in Figure 6. The nugget diameter in experiment and simulation matched and the prediction accuracy of nugget diameter was around 95%.

The stress develop after welding, residual strain generated during weld, nugget size, and contact force between two sheets for TRIP 690 are shown in Figure 7. It was observed that the prediction accuracy was around 90% for all parameters.

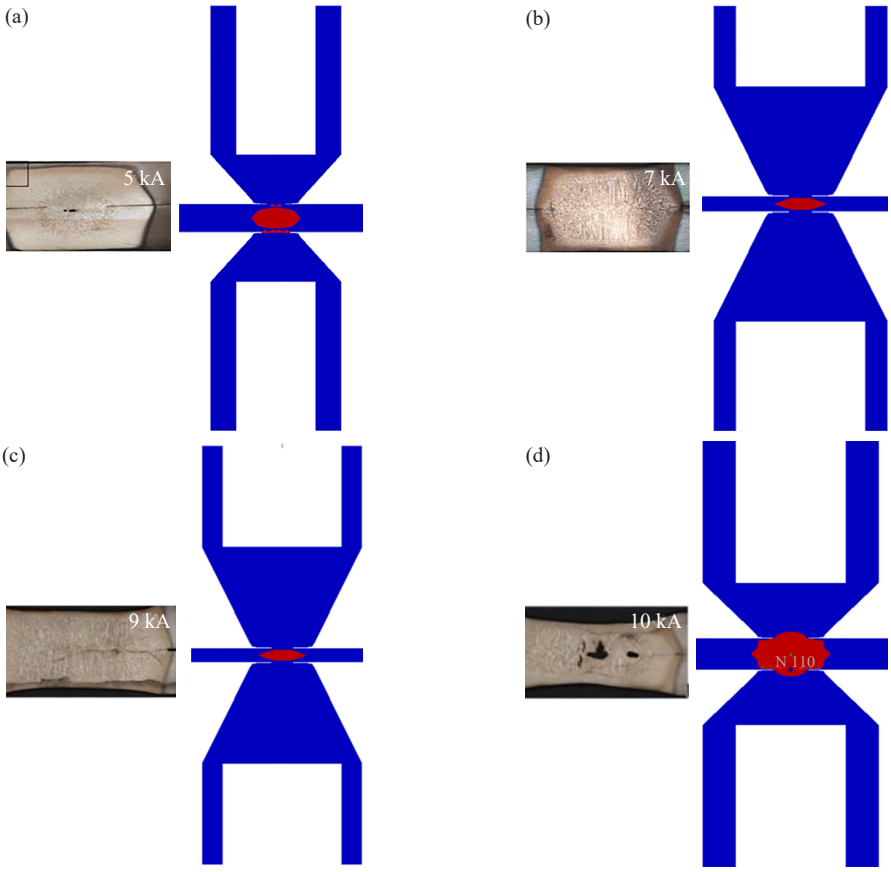

Figure 7. Comparison of experimental & simulation result of nugget size at different current for IF steel: (a) 5 kA, (b) 7 kA, (c) 9 kA, (d) 10 kA

As shown in Figure 8, with increase in current, nugget size increased. However, there is a current level above that explosion will occur. This indicated that, in case of IF steel, if the current goes above 10 kA, the explosion will happen. These simulations provide us a range current or working window to prevent material explosion.

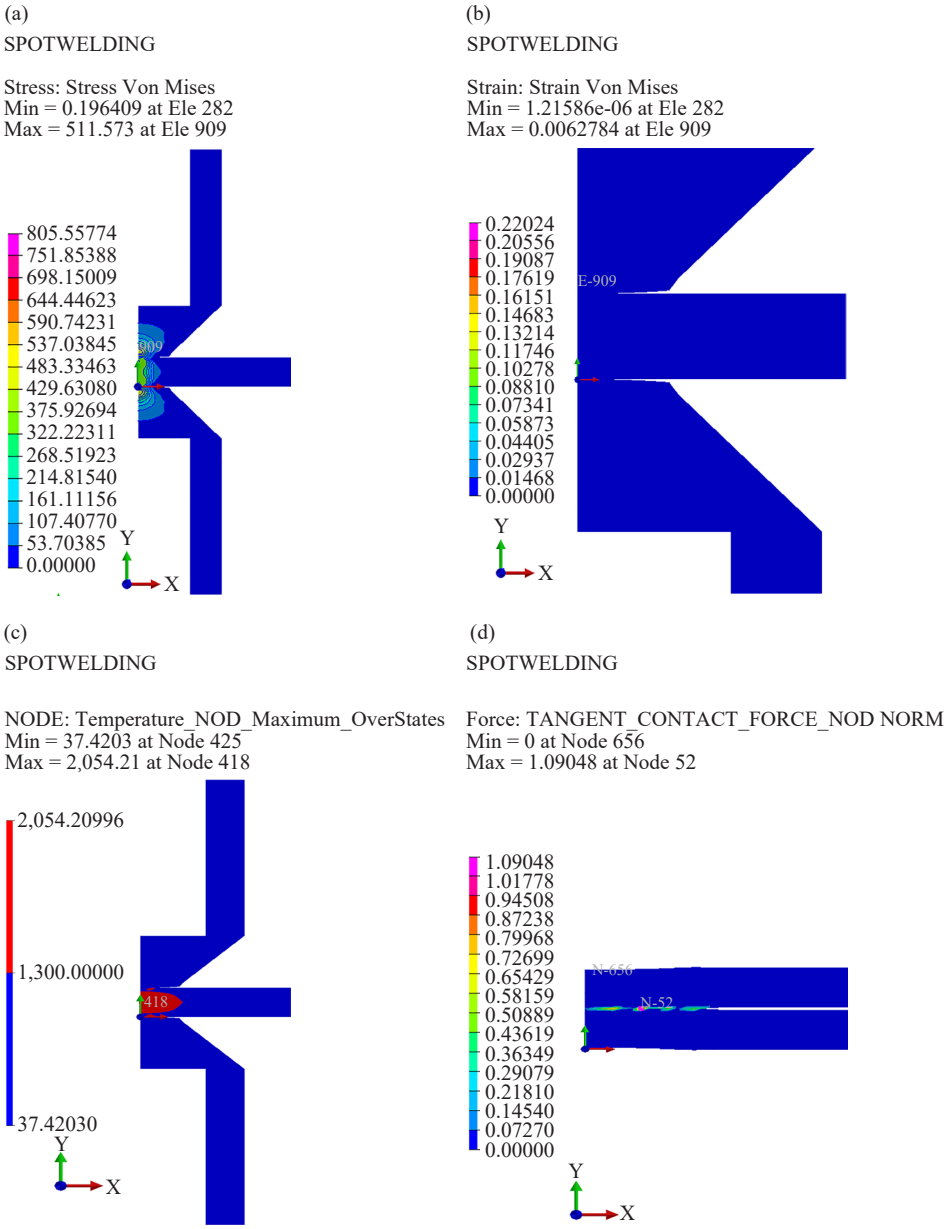

Figure 8. Different types of result obtained after SYSWELD simulation: (a) Stress Develop after welding, (b) Residual Strain generated during weld, (c) Nugget size, (d) Tangent contact force between two sheets at TRIP 690

Temperature and stress development are more pronounced at elevated current levels, as shown in Figure 9. Therefore, it is recommended to use optimum current level based on the material properties. Nugget size for TRIP 690 is compared in Figure 10.

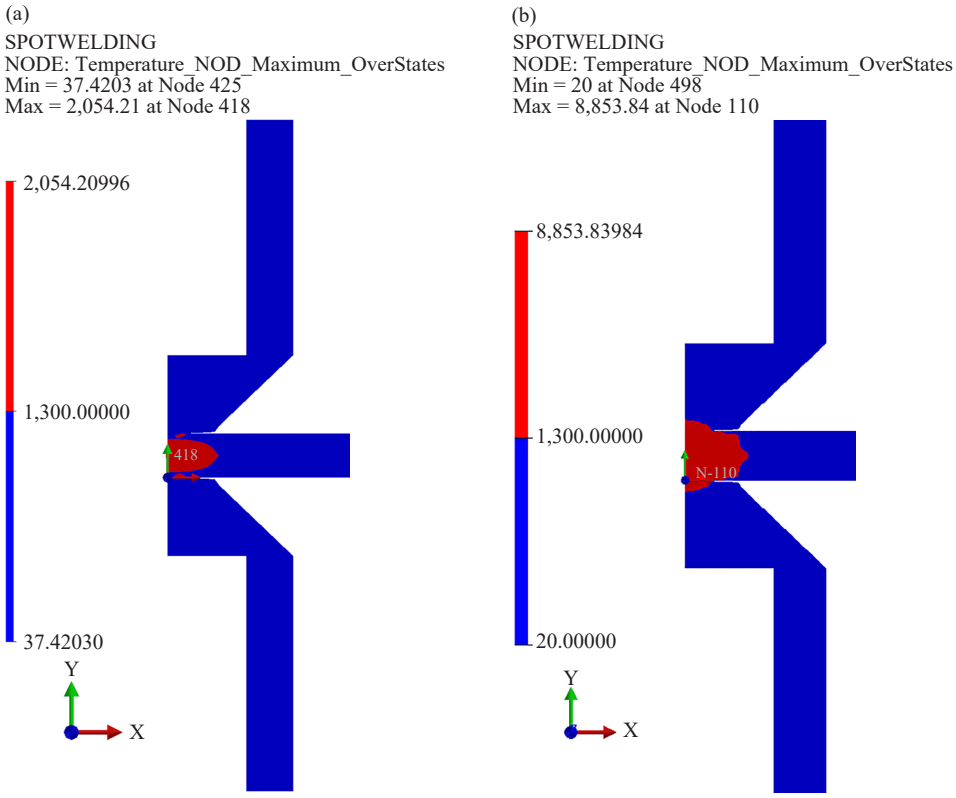

Figure 9. Temperature distribution at different current for IF steel: (a) 5 kA, (b) 10 kA

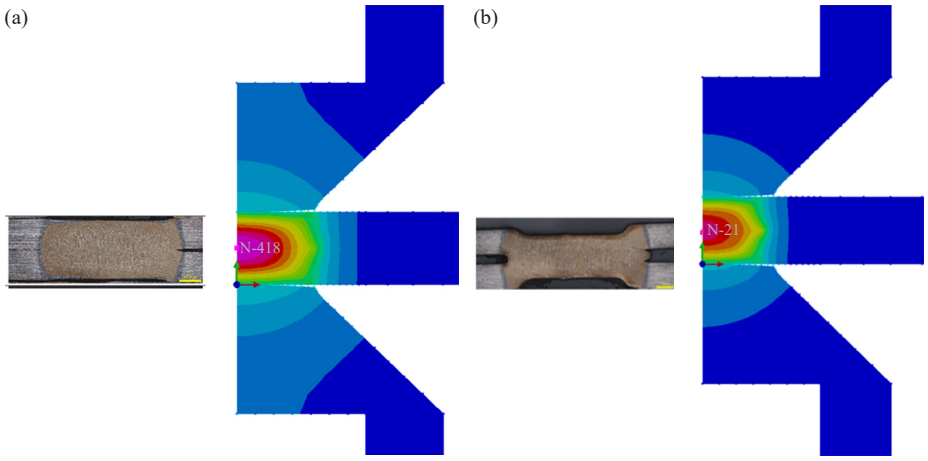

Figure 10. Comparison of experimental & simulated nugget sizes of TRIP 690 under two extreme current levels: (a) 5 kA (b) 10 kA

In Figure 11, it was observed that nugget sizes for the selected materials differ under two extreme current levels. In case of IF steel, the maximum temperature was achieved at 10 kA; however, the minimum temperature variation was observed in case of DP 980 steel. This occurs due to variation in strength and resistivity among these materials.

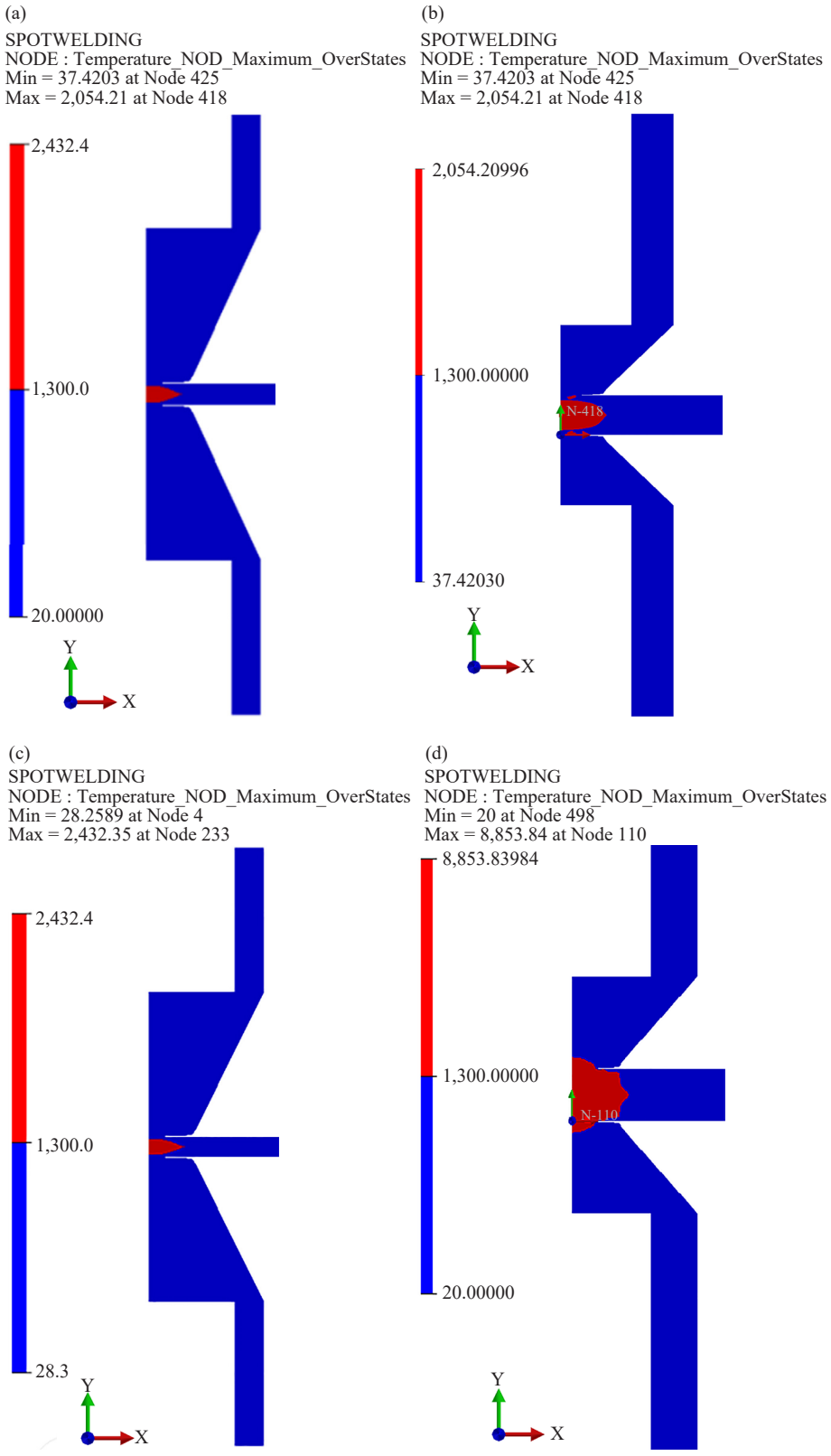

Figure 11. Nugget formation in different materials at 10 kA: (a) DP 980 (b) TRIP 690 (c) TRIP 980 (d) IF Steel

5. Conclusion

The behaviour of resistance spot welding was investigated across four commonly used automotive steel grades: IF 270, TRIP 690, DP 780, and TRIP 980. Spot welding characteristics were found to be influenced by phase transformation, with microstructure development occurring during cooling. This study provides critical current values mapping for various phenomena during resistance spot welding in automotive grades. Apart from that, these are the following outcome:

1) This study demonstrated capability of SYSWELD for spot welding and property prediction.

2) SYSWELD simulation is an alternative of physical testing that can save time and experimental costs.

3) Comparative results of experiments and simulations showed that that the explosion currents in both cases were the same.

4) Nugget size and temperature profiles can be used to predict weld strength and weld quality of materials.

5) Weldablity of a material can easily be determined using SYSWELD.

Conflict of interest

The authors declare that they have no conflict of interest regarding the research findings.

References

[1] M. Morawiec, T. Kik, S. Stano, M. Różański, and A. Grajcar, "Numerical simulation and experimental analysis of thermal cycles and phase transformation behavior of laser-welded advanced multiphase steel," *Symmetry*, vol. 14, no. 3, pp. 477, 2022.

[2] T. R. Lima, S. M. Tavares, and P. M. De Castro, "Residual stress field and distortions resulting from welding processes: numerical modelling using Sysweld," *Ciência & Tecnologia dos Materiais*, vol. 29, no. 1, pp. e56-e61, 2017.

[3] S. K. Bate, R. Charles, and A. Warren, "Finite element analysis of a single bead-on-plate specimen using SYSWELD," *International Journal of Pressure Vessels and Piping*, vol. 86, no. 1, pp. 73-78, 2009.

[4] N. Moslemi, B. Abdi, S. Gohari, I. Sudin, N. Redzuan, A. Ayob, and C. Burvill, "Influence of welding sequences on induced residual stress and distortion in pipes," *Construction and Building Materials*, vol. 342, pp. 127995, 2022.

[5] M. Pouranvari and S. P. H. Marashi, "Critical review of automotive steels spot welding process, structure and properties," *Science and Technology of Welding and Joining*, vol. 18, no. 5, pp. 361-403, 2013.

[6] Z. Han, J. Orozco, J. E. Indacochea, and C. H. Chen, "Resistance spot welding: a heat transfer study," *Welding Journal*, vol. 68, no. 9, pp. 363s-371s, 1989.

[7] H. A. Nied, "The finite element modelling of the resistance spot welding process," *Welding Journal*, vol. 63, pp. 123s-132s, 1984.

[8] C. L. Tsai, W. L. Dai, and D. W. Dickinson, "Analysis and development of a real-time control methodology in resistance spot welding," SAE International, USA, SAE Technical Paper. 910191, 1991.

[9] N. Zhong, X. Liao, M. Wang, Y. Wu, and Y. Rong, "Improvement of microstructures and mechanical properties of resistance spot welded DP 600 steel by double pulse technology," *Materials Transactions*, vol. 52, no. 12, pp. 2143-2150, 2011.

[10] T. Hsu, L. T. Wu, and M. H. Tsai, "Resistance and friction stir spot welding of dual-phase (DP 780): A comparative study," *The International Journal of Advanced Manufacturing Technology*, vol. 97, no. 5, pp. 2293-2299, 2018.

[11] H. Zhang and J. Senkara, *Resistance Welding: Fundamentals and Applications*, 2nd ed., Boca Raton, FL, USA: CRC Press, 2011.

[12] X. Sun, E. Stephens, and M. A. Khaleel, "Effects of fusion zone size and failure mode on peak load and energy absorption of advanced high strength steel spot welds under lap shear loading conditions," *Engineering Failure Analysis*, vol. 15, no. 4, pp. 356-367, 2008.